Early stages of melting in Si under nanosecond laser pulse irradiation: A timeresolved study

J. Solis and C. N. Afonso

Citation: J. Appl. Phys. **69**, 2105 (1991); doi: 10.1063/1.348968

View online: http://dx.doi.org/10.1063/1.348968

View Table of Contents: http://jap.aip.org/resource/1/JAPIAU/v69/i4

Published by the American Institute of Physics.

Early stages of melting in Si under nanosecond laser pulse irradiation: A time-resolved study

J. Solis and C. N. Afonso
Instituto de Optica, CSIC, Serrano 121, 28006 Madrid, Spain

(Received 6 August 1990; accepted for publication 12 November 1990)

Time-resolved reflectivity (TRR) measurements are performed in crystalline Si under UV and visible wavelength irradiation. The former are carried out with ArF excimer laser pulses whereas the latter are performed in micron-sized areas irradiated with Ar^+ laser pulses by means of a novel experimental setup. It is the first time that TRR measurements in the nanosecond regime are performed in micron-sized irradiated areas although they are very suitable to characterize processes in phase change optical storage and microelectronics applications. The energy density melting thresholds at both Ar^+ and ArF laser wavelengths are determined. The reflectivity values obtained for pulse fluences just above the melting threshold show that melting proceeds inhomogeneously being the near-surface region formed by a mixture of solid and liquid phases without a well-defined interface. The comparison of the results obtained with uv and visible irradiation indicates that inhomogeneous melting is a general phenomenon which does not depend on the irradiation wavelength. It is present in the early stages of the melting process and its origin is related to the phase nucleation process itself. As the laser fluence is increased, the evolution of the melt duration exhibits a "different" behavior which is related to the formation of a homogeneous molten layer on top of the surface.

I. INTRODUCTION

Time-resolved optical and electrical measurements have been widely applied to the study of pulsed laser annealing and melting of semiconductors.[1,2] Most of the reported works have dealt with rapid melting-solidification phenomena induced in Si by nanosecond laser pulses with fluences well above the melting threshold. Nevertheless the study of the material behavior at fluences around the melting threshold is important in order to characterize the early stages of the melting process.

The solid-liquid phase transition in Si is accompanied by a large increase of reflectivity (at visible and ir wavelengths) due to the metallic nature of liquid Si.[3–6] The optical transition is not abrupt and occurs instead over a finite energy range. It has been shown that maximum reflectivity values intermediate between those of crystalline and liquid Si both at the melting temperature are reached when irradiating with nanosecond pulses from visible[7] and uv[8,9] lasers. The origin of this behavior is still controversial and has been explained either in terms of the molten layer thickness[7,8] or by the formation of a non-well-defined solid-liquid interface[9] (inhomogeneous melting). The latter explanation, reported for uv irradiation results, assumes that the near-surface region of the sample does not melt homogeneously during the melt-in process but rather consists of a mixture of solid and liquid phases.

Inhomogeneous melting phenomena have been also reported to occur during the irradiation of Si with visible and near-IR laser beams.[10] It has been pointed out that the existence of an intrinsic instability at the melting threshold of Si is due to the abrupt difference between the optical properties of the solid and the liquid material at these wavelengths. The power required to bring the solid material to the melting point (Tm) is then much lower than the one required to keep the liquid at Tm. For powers between these two extremes, the material has to remain at Tm and so its average reflectivity has to be intermediate between those of the liquid and the solid. It yields the formation of a non-well-defined solid-liquid interface in which solid and liquid material coexist in the homogeneously irradiated material.[10,11] This "optical induction" model for inhomogeneous melting has been used[11] to account for the existence of laser induced periodic surface structures (LIPSS)[12] when irradiating semiconductors with fluences just above the melting threshold. However this explanation is not valid for the case of uv irradiation[9] since at these wavelengths the optical properties of liquid and solid Si are not too different. Other explanations like inhomogeneities in the spatial distribution of the laser radiation, microscopic imperfections in the sample surface or the phase nucleation process itself were proposed.

This work presents a time-resolved optical study of the processes induced in *c*-Si by irradiation with nanosecond laser pulses. Its aim is to characterize by means of optical measurements the processes induced in Si by laser pulses with fluences in the neighborhood of the melting threshold in order to obtain information about the early stages of melting and the liquid-phase nucleation process. We have used nanosecond laser pulses from two different lasers in order to compare the results obtained with visible (Ar^+ laser) and uv (ArF excimer laser) light irradiation. The former laser is used to induce melting in micron-sized areas whereas the latter is used to irradiate macroscopic ones. In both cases the optical probe is a HeNe laser.

To our knowledge, this is the first reported experiment in which time-resolved optical measurements are used to characterize irradiation processes induced by nanosecond

 0021-8979/91/042105-07$03.00

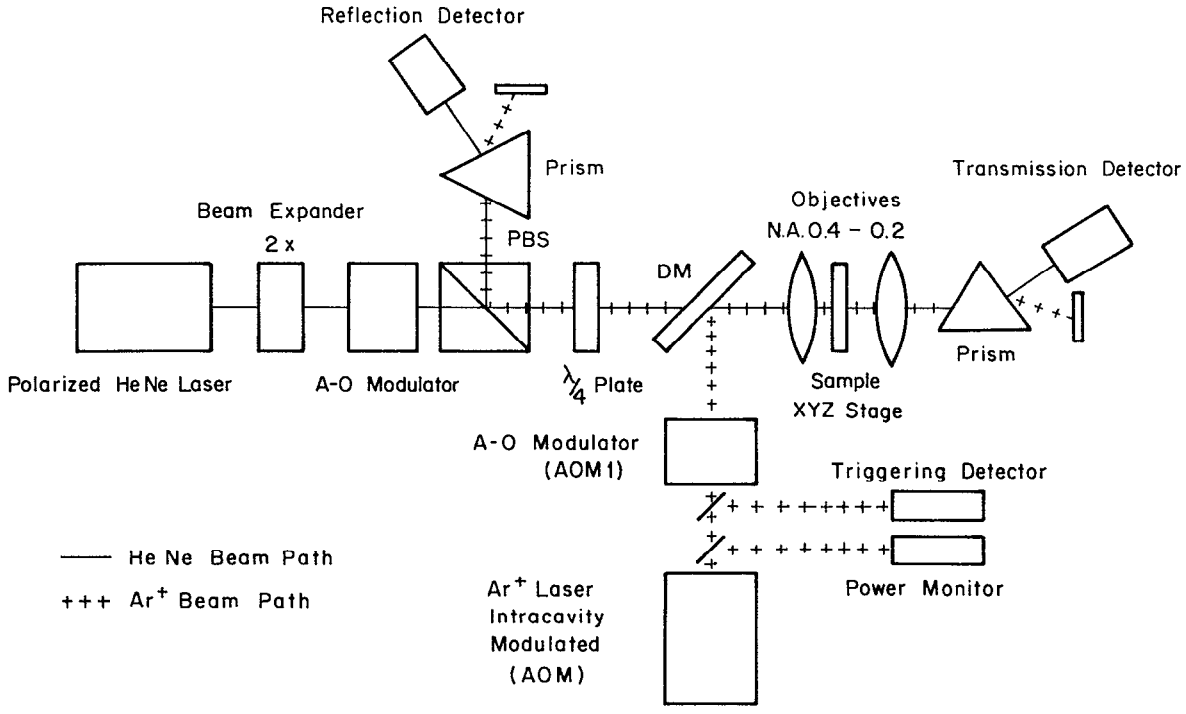

FIG. 1. Schematical drawing of the experimental setup used to perform TRR measurements on micron-sized areas when irradiating with Ar^+ laser pulses.

pulses both at Ar^+ laser wavelengths and at micron-sized areas by focused laser beams. The use of time-resolved optical measurements to characterize the processes induced by focused laser beams has been reported before for laser pulses in microsecond or longer regimes[13,14] and is a very useful technique for microelectronics and optical storage applications.

Melting thresholds at both pump wavelengths are determined. The reflectivity values measured for fluences just above the melting threshold show clearly that, independently of the irradiation wavelength (uv or visible radiation), the melting process proceeds inhomogeneously, with a non-well-defined solid-liquid interface. It will be shown that this inhomogeneity is a characteristic of the early stages of the melting process.

II. EXPERIMENTAL PROCEDURE

The samples, *N*-type 0.2 Ω/cm Si ⟨111⟩ wafers, are irradiated with nanosecond pulses provided either by an intracavity modulated Ar^+ laser or an ArF excimer laser. In both cases a pulsed HeNe laser (632.8 nm) is used to monitor the reflectivity of the material during irradiation.

The experimental setup used to perform the irradiations and time-resolved optical measurements when irradiating with Ar^+ laser pulses is schematically shown in Fig. 1. Both pump and probe beams are focused at normal incidence onto the sample to a 1/e beam radii of 4 and 1.7 μm, respectively. The Ar^+ laser is operated in multiline mode ($\lambda = 2488$, 514 nm) in order to obtain its maximum output power. An intracavity acousto-optic modulator (AOM) allows to obtain Gaussian 18 ns ($2\times 1/e$ intensity decay) pump pulses or cw radiation. The latter can be pulsed by means of an external acousto-optic modulator (AOM1) to produce square pump pulses with pulselengths ranging from 200 ns to cw. The use of AOM1 is also necessary to cut off a low-power cw spurious radiation which comes out from the laser when it operates at 18 ns. The ratio from the spurious signal to the pulse peak power is typically $1/10^5$–10^6. Depending on the material, this background can be large enough to induce a preannealing effect when it is focused on the sample during periods of time in the millisecond regime. In order to minimize this effect, the external acousto-optic modulator is switched on during 160 ns, being the intracavity generated pulse centered at this time interval.

The probe pulse power and length are suitably adjusted in order to optimize the signal-to-noise ratio and to avoid any appreciable heating or damage in the samples due to a long duration cw annealing.[15] The probe pulse is triggered before the pump pulse reaches the sample and its pulse length is usually set to be at least ten times the pump pulse length. With this pulse scheme, the optical properties of the material both before and after irradiation are monitored. It is also ensured that the transient process induced by the irradiation is completed. In the present research we use 2800 ns square pulses with a power at the sample site of 1 mW. The temperature increase induced by this probe pulse is estimated to be lower than 5 K per absorbed

mW.[16–18]

The pump and probe beams are overlapped at the surface of a dielectric mirror (DM) to be then focused concentrically on the sample at normal incidence. The latter is mounted in a XYZ micropositioning stage and moved to a new position after each laser shot. A high-dispersive spectroscopic prism is used to eliminate any residual contribution of the pump pulse to the reflectivity signal. As can be seen in Fig. 1 the experimental setup can be also used to perform time-resolved transmission measurements during the irradiation of semi-transparent materials. The use of normal incidence for both pump and probe beams as well as the excellent signal-to-noise ratio achieved allows a resolution both in the reflected and the transmitted light measurements better than 0.5%.

The detection of the optical transients is performed by means of fast 500-ps risetime compact *p-i-n* detectors. Their signals are filtered with a narrowband notch filter in order to suppress the 500 MHz modulation produced by mode competition in the HeNe laser. The optical transients are finally recorded by means of a 500-MHz transient digitizer (Tektroniks 7912 AD) remote controlled by a computer. A fast detector is used to trigger the digitizer by the pump pulse itself. The position of the transients with respect to the irradiation pulse is then determined within ± 1 ns.

In the present research we have used 18-ns pump pulses with energies ranging from 74 to 164 nJ at the sample site. Taking into account the pump beam Gaussian energy distribution, the conversion of these values to fluences leads[19] to energy density values at the maximum ranging fron 148 to 328 mJ/cm^2. Several transients are recorded at different sample positions for each energy density value.

The uv irradiations are performed with 12 ns (FWHM) laser pulses provided by an ArF excimer laser (Questek 2440, $\lambda = 2193$ nm). A 104-mm focal length cylindrical lens is used to focus the laser beam over a 0.75×6.75 mm^2 area. The probe beam is incident at 12° off the surface normal and is focused to $a \approx 160$ μm $1/e$ beam radius at the center of the irradiation area. Similarly to what is already described for the Ar^+ laser experiments, it is pulsed to 2800 ns. The pump beam energy distribution over the probed area is homogeneous within 5% and the energy density values are ranged from 475 to 1283 mJ/cm^2. The detection and signal processing equipment is identical to that already described.

III. RESULTS

Figure 2 shows the reflectivity of Si as a function of time for several values of the pulse energy density when irradiating with Ar^+ (a) or excimer (b) pump pulses. In both cases the time scale origin ($t = 0$) is taken at the pump pulse maximum. As a consequence of the irradiation, the reflectivity increases to reach a maximum value (R_{max}) whose position depends slightly on the pulse energy density (J). The measured initial and final reflectivity levels are equal to that of *c*-Si at room temperature within the experimental resolution ($R = 0.35$).[20] The apparent difference observed after irradiation in Fig. 2 comes from the fact that the material requires times about 100 ns to reach equilibrium after the maximum of the pump pulse. This has been confirmed following the evolution of the transients for times longer than 200 ns as well as measuring statically the reflectivity values before and after the irradiation. To ease the comparison between the transients induced by the Ar^+ and the excimer laser, Fig. 2(c) includes transients induced by both lasers. Although the energy densities used in each case are different, they correspond to similar induced effects.

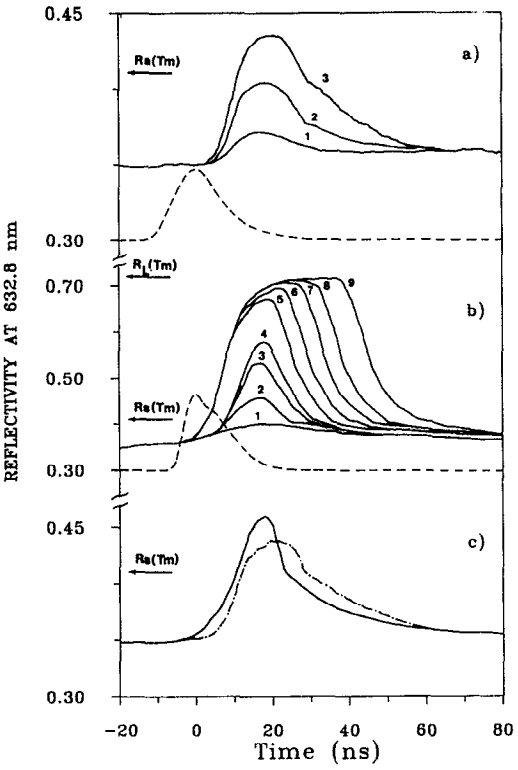

FIG. 2. TRR transients induced by Ar^+ (a) and excimer (b) laser pulses. The pump pulse is included (- - - - -) and its maximum is taken as the origin of the time scale. The transients are induced by 148 (1), 208 (2) and 268 (3) mJ/cm^2 laser pulses from the Ar^+ laser (a) and 546 (1), 665 (2), 760 (3), 807 (4), 863 (5),940 (6), 1093 (7), 1156 (8) and 1283 (9) mJ/cm^2 laser pulses from the excimer laser (b). The transients plotted in (c) are obtained under irradiation with 208 mJ/cm^2 (-· -·) and 665 mJ/cm^2 (—) pulses from Ar^+ and excimer lasers, respectively. R_s(Tm) and R_L(Tm) denote the reflectivity of crystalline Si and liquid Si at the melting temperature.

A. Ar^+ laser irradiations

For J values above a threshold (≈ 200 mJ/cm^2), R_{max} is reached at a constant time ($t \approx 18$ ns) and the cooling tail of the transients exhibits an inflection in the neighborhood of the pump pulse end. The evolution of the reflectivity value both at the inflection (R_{inf}) and the maximum (R_{max}) as a function of J can be seen in Fig. 3. Figures 2(a) and 3 suggest the existence of three different regimes as the energy density increases. They are evidenced by the slope changes in Fig. 3.

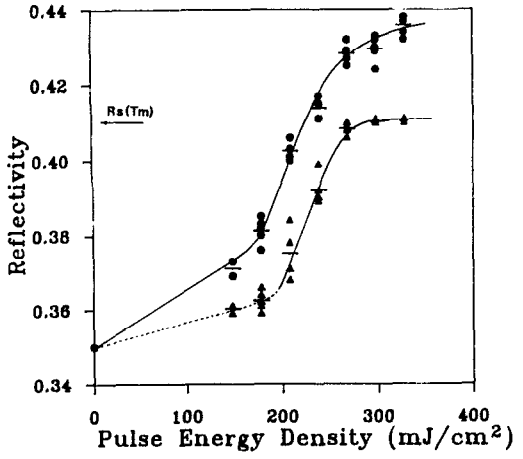

FIG. 3. Maximum transient reflectivity (R_{max}) (●) and reflectivity value at the inflection (R_{inf}) (▲) vs Ar^+ laser fluence when irradiating with Ar^+ laser pulses. The plotted R_{inf} values for $J < 200$ mJ/cm^2 [absence of inflection, (------)] correspond to the reflectivity value at the pump pulse end. The solid lines are guidelines and the bars denote average values.

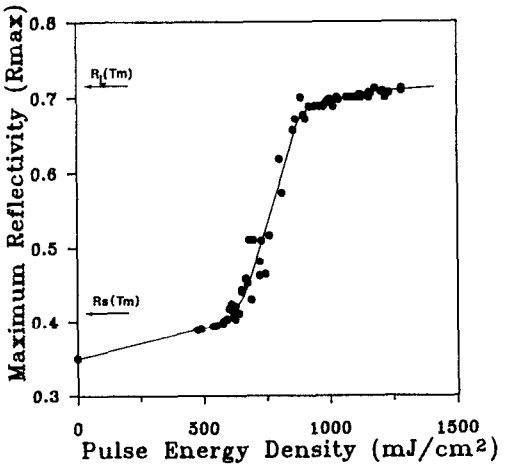

FIG. 4. Maximum transient reflectivity (R_{max}) vs laser fluence when irradiating with excimer laser pulses. The solid line is a guideline.

The first regime corresponds to $J \leqslant 180$ mJ/cm^2 and is characterized by R_{max} values always below the reflectivity of solid Si at the melting point [$R_s(\mathrm{Tm}) = 0.41$].[21] An approximately linear behavior of R_{max} vs J is observed. The shape of the transients belonging to this regime is identical to that included in Fig. 2(a) for $J = 148$ mJ/cm^2. No inflection is seen in the cooling tail of the transients.

The second regime is characterized by the rapid increase of both R_{max} and R_{inf} as J increases within the 180–260 mJ/cm^2 interval and by the fact that R_{max} is reached ≈ 18 ns after the pump pulse maximum independently of J. The R_{max} values are around that of solid c-Si at the melting point but well below that of liquid Si at the melting temperature [$R_L(\mathrm{Tm}) = 0.70$–0.73].[5,22] All the recorded transients present the inflection at the neighborhood of the pump pulse end as can be seen in Fig. 2(a) in the typical transient belonging to this regime ($J = 208$ mJ/cm^2).

The third regime which corresponds to $J \geqslant 260$ mJ/cm^2 starts when the reflectivity value at the inflection point reaches a constant value equal to $R_s(\mathrm{Tm})$ (see Fig. 3). The shape of the transients is similar to that observed in the 180–260 mJ/cm^2 interval but now R_{max} is always above $R_s(\mathrm{Tm})$ and increases slowly as J increases (Fig. 3). A typical example of this regime is the transient obtained with 268 mJ/cm^2 in Fig. 2(a). R_{max} values close to $R_L(\mathrm{Tm})$ are not reached in the studied energy density range (148–328 mJ/cm^2) whose upper limit corresponds to the maximum output power of the used Ar^+ laser.

B. Excimer laser irradiations

Similar to what was described for the Ar^+ laser irradiations and for J values above a given threshold (≈ 650 mJ/cm^2 in this case), R_{max} is reached at a constant time (≈ 15 ns) and the cooling tail of the transients exhibits an inflection when the reflectivity reaches the value $R_s(\mathrm{Tm})$ [Fig. 2(b)]. This slope change is clearer in an expanded scale [see Fig. 2(c)].

The R_{max} values induced by excimer laser pulses as a function of J are plotted in Fig. 4. For fluences below ≈ 650 mJ/cm^2, R_{max} has a linear dependence on J and it is always below $R_s(\mathrm{Tm})$. For fluences above ≈ 850 mJ/cm^2 the induced R_{max} values are very close to $R_L(\mathrm{Tm})$ and the effect of increasing the pulse energy density is to increase the melt duration without any significant changes in R_{max} (see Fig. 4). The shape of the transients for these fluences well above the melting threshold is similar to that which has been widely reported in the literature. Between these two extremes (650 and 850 mJ/cm^2) R_{max} increases monotonically. The maximum transient reflectivity tends to the value 0.715 in excellent agreement with the value reported for $R_L(\mathrm{Tm})$ by Jellison and co-workers.[22] The width of the transition from the reflectivity of solid Si to that of liquid Si both at the melting temperature is ≈ 200 mJ/cm^2.

IV. DISCUSSION

A. Optical transients and melting thresholds

When the excimer laser is used as the pump beam, the intensity distribution within the probed region is nearly homogeneous. In the case of the Ar^+ laser irradiations both the size and the Gaussian profile of the pump beam may influence the measured reflectivity values. The TRR transients induced by excimer laser pulses are then an adequate reference for the interpretation of the transients induced by Ar^+ laser pulses in micron-sized areas and will be therefore analyzed first.

It is clear from Fig. 4 that excimer laser fluences above ≈ 650 mJ/cm^2 yield R_{max} values above $R_s(\mathrm{Tm})$ and therefore the material undergoes a solid–liquid phase transition. The inflection observed in the cooling tail of the transients at $R = R_s(\mathrm{Tm})$ [Fig. 2(c)] is then clearly related to the total disappearance of the liquid phase followed by the cooling of the solid material. The obtained energy density melting threshold [Jm(193 nm) = 650 mJ/cm^2] is in very

good agreement with that reported by Jellison and co-workers[9] at 248 nm. Since the reflectivities of crystalline Si at 193 and 248 nm are very similar (0.68–0.69 versus 0.66–0.68),[23] no appreciable differences are expected between the energy density melting thresholds at both wavelengths. The difference between our value and that reported by Foulon and co-workers[8] at 193 nm (395–417 mJ/cm^2) could be related to the differences in the pump pulse length and shape used.[24] For fluences $J < Jm$, the linear behavior of R_{max} (Fig. 4) can be roughly explained by the well-known linear behavior of the reflectivity of Si with temperature.[21] Nevertheless, a precise calculation should take into account the temperature dependence of the absorption coefficient at the pump wavelength. Finally, it is clear that for fluences above 850 mJ/cm^2 R_{max} tends to R_L(Tm) indicating the formation of a homogeneous molten layer on the sample surface. The origin of the reflectivity values intermediate between R_s(Tm) and R_L(Tm) will be discussed in Sec. IV B.

The energy density melting threshold at Ar^+ laser wavelengths can be estimated in a first approach as 268 mJ/cm^2 since this is the first experimental value which leads to R_{max} values significantly higher than R_s(Tm). Besides, for fluences higher than $\approx$260 mJ/cm^2, R_{inf} reaches a saturation value equal to R_s(Tm) (Fig. 3) similarly to what is observed under irradiation with excimer laser pulses above the melting threshold. It can be then concluded that Ar^+ laser fluences above $\approx$260 mJ/cm^2 induce melting.

However, the characteristic inflection in the cooling tail of the transients is first observed for Ar^+ laser fluences in the 180–260 mJ/cm^2 but with R_{inf} values below R_s(Tm). In order to understand this feature, two factors related to the characteristics of the experimental setup have to be taken into account: (a) The material is not homogeneously irradiated because of the Gaussian distribution of the Ar^+ laser beam intensity profile. (b) The pump and the probe beams are both focused on micron-sized areas. Depending on the energy density, the probed area may contain solid and liquid phases with a radial distribution and the measured reflectivity value would be then a weighted average of the reflectivities of the solid and the liquid material. This melt lateral extension effect in TRR measurements has been earlier reported for a similar experimental setup. It was shown there[13] that as the irradiation power increases, the melt radius increases as well and the measured reflectivity value tends to that of the liquid phase. A minimum melt radius of $r_c \approx 2.1\ r_0$ ($r_0 = 1/e$ radius of the probe beam) is found to be necessary to probe only melted material.

From the excimer laser studies, it is demonstrated that when melting occurs, an inflection is observed in the cooling tail of the transients. The presence of this inflection in the transients obtained with Ar^+ laser fluences between 180 and 260 mJ/cm^2 proves that the melting threshold is within this fluence regime. If we take into account the above discussion concerning the melt lateral extension effects, we can conclude that fluences below 260 mJ/cm^2 (and above 180 mJ/cm^2) induce melting but the lateral extension of the molten region is not enough to "saturate" the probe beam. Furthermore, we have seen experimentally that the first energy density value at the maximum able to induce melting in a circle of radius r_c is 268 mJ/cm^2. The average energy density of this pulse over the circle is 183 mJ/cm^2 and therefore any pulse with a maximum energy density above 183 mJ/cm^2 but below $\approx$260 mJ/cm^2 will induce melting but only in part of the probed area. This reasoning is in very good agreement with the experimental data. The presence of the liquid phase is evidenced by the appearance of the inflection together with the sharp increase of R_{max} at 208 mJ/cm^2 which is the first experimental value above 183 mJ/cm^2. It can be then concluded that the energy density melting threshold of Si at Ar^+ laser wavelengths must be in the 180–200 mJ/cm^2 interval.

B. Reflectivity levels just above the melting threshold and inhomogeneous melting

In order to simplify the discussion concerning the optical properties of the irradiated material, in this part we will refer only to those irradiation conditions in which melt lateral extension effects are not present.

The comparison of the TRR transients obtained for fluences above the melting threshold for both pump wavelengths points out that the existence of maximum reflectivity levels (R_{max}) between R_s(Tm) and R_L(Tm) should obey the same origin. It has then to be independent of the pump pulse wavelength.

For the case of the irradiations with Ar^+ laser pulses, the absorption length of the solid material near the melting point is about 100 nm. This value is much longer than the skin penetration depth of the liquid phase at 632.8 nm. Therefore the melt depth induced by a pulse with $J > 260$ mJ/cm^2 should be enough to produce a "thick" liquid layer as measured by the probe beam. For instance, if the pulse were able to induce melting in a depth of just 10 nm, the probe beam would record a reflectivity level of 88% of that of a bulk liquid[8] in disagreement with the experimental observations. This estimation gives grounds for inferring that the existence of R_{max} levels above R_s(Tm) but well below R_L(Tm) is not related to a melt depth effect.

A further argument, valid for both excimer and Ar^+ laser irradiations, can be provided. If the intermediate reflectivity values were caused by a melt depth effect, then the melt duration should continuously approach to zero as the pulse energy decreases. Nevertheless melt durations (τ_m) below $\approx$15 ns are not experimentally observed. The discontinuity of τ_m as a function of J can be clearly appreciated in Fig. 5 for the case of irradiations with excimer laser pulses. It is not straightforward to determine the melt duration induced by the Ar^+ laser irradiation as a function of the pulse energy density in the 180–260 mJ/cm^2 interval since the transients in this regime are influenced by melt lateral extension effects. However an underestimation of the melt onset can be done assuming that melt starts when the reflectivity equals the value at the inflection in the cooling tail of the first transient in this latter regime. Using this criterion, it is seen that the melt duration induced by

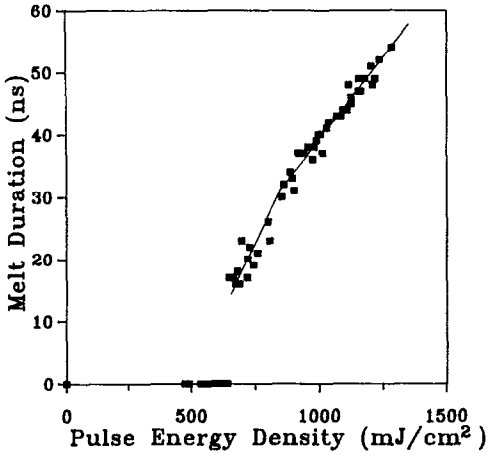

FIG. 5. Melt duration vs excimer laser fluence. The solid line was obtained from the best linear fits of the experimental data above the discontinuity. It shows two different slopes.

Ar^+ laser pulses with fluences above the melting threshold is also never lower than $\approx$20 ns.

Earlier time resolved ellipsometry experiments during laser irradiation of *c*-Si and *c*-Ge with an excimer laser (KrF = 248 nm) have given results consistent with a nonhomogeneous melt-in process.[9] The front surface region is considered as a mixture of solid and liquid phases where the fraction of liquid and its thickness are time dependent. The optical transients obtained for energy densities slightly above the melting threshold showed two important features: (a) The melt duration was never lower than $\approx$20 ns and (b) The maximum transient reflectivity was reached at a constant time ($\approx$15 ns) after the pump pulse maximum. Both features are present in our results, when irradiating with excimer and Ar^+ lasers. We can then conclude that the existence of reflectivity levels between $R_s(\mathrm{Tm})$ and $R_L(\mathrm{Tm})$ is related to an inhomogeneous melting process.

Since similar results are obtained when using visible and uv laser irradiation, inhomogeneous melting has to be a general phenomenon which is present in the early stages of melting. The origin of inhomogeneous melting phenomena in Si irradiated at visible and near IR wavelengths has been related to the important differences between the reflectivity and the optical absorption of the solid and the liquid phases.[10,11] This explanation can be discarded comparing the results obtained with visible irradiation (Ar^+ pump pulses) to those obtained by irradiation with uv light (ArF pump pulses) at which there are not significant differences between the optical properties of the solid and the liquid material. On the other hand, the absence of hot spots in the Ar^+ laser intensity distribution allows to discard inhomogeneities in the laser spatial distribution[9] as the mechanism responsible for inhomogeneous melting. The most likely explanation is then to consider the inhomogeneity of the early stages of melting as a consequence of the liquid-phase nucleation itself. Results from pulsed Raman experiments on *c*-Si irradiated at 530 nm[25] as well as time-resolved ellipsometry experiments,[9] indicate the existence of a minimum time for developing a homogeneous molten layer when irradiating at fluences well above the melting threshold and give further support for this conclusion.

The evolution of the melt duration (τ_m) as a function of the pulse energy density for the excimer laser irradiations (Fig. 5) points out the existence of two "different" melting thresholds. The first one which is coincident with the strong discontinuity of τ_m at $\approx$650 mJ/cm^2 ($\approx$200 mJ/cm^2 for Ar^+ laser irradiation) should correspond to the energy required to nucleate the liquid phase. The second one, evidenced by the slope change at 850 mJ/cm^2, corresponds to the energy density required to induce a homogeneous molten layer on top of the surface.

V. CONCLUSIONS

A novel experimental setup has been developed in order to obtain high-sensitivity time resolved optical measurements on micron-sized laser irradiated areas. The energy density melting threshold of crystalline Si at Ar^+ laser wavelengths (488, 514 nm) has been determined to be 180–200 mJ/cm^2. TRR measurements during pulsed excimer laser (193 nm) irradiation have been also performed and yield an energy density melting threshold of 650 mJ/cm^2.

In both cases (uv and visible irradiation) the reflectivity levels measured for fluences slightly above the melting threshold are consistent with an inhomogeneous melting process. It is characterized by the formation of a zone in the near surface region in which liquid and solid phases coexist without a well-defined interface.

From the comparison of the results obtained from uv and visible laser irradiation it is concluded that inhomogeneous melting is a general phenomenon. It is present in the early stages of the melting process and does not depend on the irradiation wavelength. Its origin is related to the liquid-phase nucleation process itself. The evolution of both the maximum transient reflectivity and the melt duration as a function of the pulse energy shows the existence of two "different" melting thresholds related to the minimum energy density necessary for the nucleation of the liquid phase and to the minimum energy density required to develop a homogeneous molten layer on top of the surface.

ACKNOWLEDGMENTS

We greatly acknowledge Dr. F. Catalina (Instituto de Optica, CSIC, Spain) for many helpful discussions. This work was partially supported by CICYT (Spain) under project MAT88-0437.

[1] P. S. Peercy, M. O. Thompson, and J. Y. Tsao, Mater. Res. Soc. Symp. Proc. **74**, 15 (1987).
[2] S. R.Stiffler and M. O. Thompson, Appl. Phys. Lett. **56**, 1025 (1990).
[3] W. R. Sooy, M. Geller, and D. P. Bortfeld, Appl. Phys. Lett. **5**, 54 (1964).
[4] D. H. Auston, C. M. Surko, T. N. C. Venkatesaan, R. F. Slusher, and J. A. Golovchenko, Appl. Phys. Lett. **33**, 437 (1978).
[5] K. M. Shvarev, B. A. Baum, and P. van Gel'd, High Temp. **15**, 718 (1985).

[6] D. H. Lowndes, G. E. Jellison Jr., and R. F. Wood, Phys. Rev. B **26**, 6747 (1982).
[7] D. H. Lowndes, R. F. Wood, and R. D. Westbrook, Appl. Phys. Lett. **43**, 258 (1983).
[8] F. Foulon, E. Fogarassy, A. Saloui, C. Fuchs, S. de Unamuno, and P. Siffert, Appl. Phys. A **45**, 361 (1988).
[9] G. E. Jellison Jr., D. H. Lowndes, D. N. Mashburn, and R. F. Wood, Phys. Rev B **34**, 2407 (1986).
[10] W. G. Hawkings and D. K. Biegelsen, Appl. Phys. Lett. **42**, 358 (1983).
[11] M. Combescot, S. Bok, and G. Benoit á la Guillaume, Phys. Rev B **29**, 6393 (1984).
[12] J. E. Sipe, J. F. Young, J. S. Preston, and H. M. van Driel, Phys. Rev. B **27**, 1141 (1983); J. F. Young, J. S. Preston, H. M. van Driel, and J. E. Sipe, Phys. Rev. B **27**, 1155 (1983); J. F. Young, J. E. Sipe, and H. M. van Driel, Phys. Rev. B **30**, 2001 (1984).
[13] C. N. Afonso, J. Solis, and F. Catalina, Appl. Surf. Sci. **43**, 171 (1989).
[14] C. J. Van der Poel, J. Mat. Res. **3**, 126 (1988).
[15] C. N. Afonso, F. Catalina, and J. Solis, Mater. Sci. Eng. B **7**, 169 (1990).
[16] M. Lax, J. Appl. Phys. **48**, 39 (1978).
[17] M. Lax, Appl. Phys. Lett **33**, 786 (1978).
[18] Y. I. Nissim, A. Lietoila, R. B. Gold, and J. P. Gibbons, J. Appl. Phys. **51**, 274 (1980).
[19] I. W. Boyd *Laser Processing of Thin Films and Microstructures*, Springer Series in Materials Science (Springer, Berlin, 1987), Vol. 3.
[20] G. E. Jellison Jr. and F. A. Modine, Phys. Rev. B **27**, 7466 (1983).
[21] G. E. Jellison Jr. and H. H. Burke, J. Appl. Phys. **60**, 841 (1986).
[22] G. E. Jellison Jr. and D. H. Lowndes, Appl. Phys. Lett. **47**, 718 (1985).
[23] *Handbook of Optical Constants of Solids*, edited by E. D. Palik (Academic, New York, 1985).
[24] P. Baeri and S. U. Campisano, in *Laser Annealing of Semiconductors*, edited by J. M. Poate and J. W. Mayer (Academic, New York, 1982), Chap. 4.
[25] G. Waartmann and D. von der Linde, J. Physique C5 **40**, Suppl. 10, 107 (1983).